J Neurosurg (Suppl) 105:86–90, 2006

Gamma Knife surgery for metastatic brain tumors without prophylactic whole-brain radiotherapy: results in 1000 consecutive cases

Toru Serizawa, M.D., Ph.D., Yoshinori Higuchi, M.D., Ph.D., Junichi Ono, M.D., Ph.D., Shinji Matsuda, M.D., Ph.D., Osamu Nagano, M.D., Yasuo Iwadate, M.D., Ph.D., and Naokatsu Saeki, M.D., Ph.D.

Gamma Knife House, Departments of Neurosurgery and Neurology, Chiba Cardiovascular Center, Ichihara; and Department of Neurological Surgery, Graduate School of Medicine, Chiba University, Chiba, Japan

Object. The authors analyzed the effectiveness of Gamma Knife surgery (GKS) for metastatic brain tumors without adjuvant prophylactic whole-brain radiotherapy (WBRT). Salvage GKS was performed as the sole treatment for new distant lesions.

Methods. Among 1127 patients in whom new brain metastases had been diagnosed, 97 who met one or more of the following three criteria were excluded from the study: any surgically inaccessible huge (≥ 35 mm) lesion; tumor number and size requiring an internal skull dose exceeding 10 J; or symptomatic carcinomatous meningitis. Thus, 1030 consecutive patients formed the basis for this study. Huge tumors were totally removed, whereas smaller lesions were treated with GKS. No adjuvant WBRT was given prior to GKS, and new distant lesions were appropriately retreated with GKS. Overall, neurological and new lesion–free survival curves were calculated and the prognostic values of covariates were obtained. In total, 1853 separate GKS sessions were required to treat 10,163 lesions.The patients' median overall survival period was 8.6 months. Neurological survival and new lesion–free rates at 1 year were 89.1 and 49.3%, respectively. In a multivariate analysis, the significant factors for poor prognosis were the development of more than four new brain metastases and active extracranial disease.

Conclusions. In meeting the goal of preventing neurological death and maintaining activities of daily living for patients with brain metastases, GKS alone provides excellent palliation without prophylactic WBRT. New distant lesions were quite well controlled with GKS salvage treatment alone.

Key Words • metastatic brain tumor • stereotactic radiosurgery • Gamma Knife surgery • whole-brain radiotherapy • neurological survival

We previously reported on the effectiveness and limitations of GKS without the addition of prophylactic WBRT, especially in patients with lung cancer.[5–7] The present study provides a rather large data set based on treatment with GKS alone for brain metastases from various primary cancers. All cancer types were treated according to the same protocol, with the focus being on new distant lesions and salvage GKS.

Clinical Material and Methods

Among 1127 patients in whom new brain metastases had been diagnosed, 97 who met one or more of the following three criteria were excluded from the study: any patient with a surgically inaccessible huge (≥ 35 mm) lesion; any patient with a tumor number and size requiring a TSID exceeding 10 J; or any patient with symptomatic carcinomatous meningitis. Thus, 1030 consecutive patients formed the basis for this study. Huge tumors were totally removed, whereas smaller lesions were treated with GKS. No adjuvant WBRT was given prior to GKS. New distant lesions, detected on MR imaging performed every 2 to 3 months, were appropriately retreated with GKS, if the patient's condition allowed. The TSID calculated with the Leksell Gamma Plan (Elekta Instruments, Norcross, GA) for each radiosurgical procedure was less than 10 J, thus preventing acute brain swelling, as previously reported.[5–7] The patients' primary physicians determined chemotherapy protocols. Neurological evaluations and Gd-enhanced MR imaging were performed every 2 to 3 months until the patient's KPS score was below 70. Thereafter, enhanced MR images were obtained at the primary hospital for as long as possible and sent to us for evaluation. The dates and causes

Abbreviations used in this paper: ADL = activities of daily living; CSF = cerebrospinal fluid; HR = hazard ratio; KPS = Karnofsky Performance Scale; MR = magnetic resonance; NLFS = new lesion–free survival; NS = neurological survival; OS = overall survival; QS = quality of survival; TSID = total skull internal dose; WBRT = whole-brain radiotherapy.

of death and progression of impaired ADL were documented by the patients' primary physicians. Control of the GKS-treated lesion was defined as the absence of any significant increase in tumor diameter (< 20%). Thallium-201 chloride single-photon emission computed tomography, as previously reported,[8] was used to differentiate tumor recurrence from radiation injury. The definitions of tiny, small, medium, and large lesions were as follows: less than or equal to 1 cm, greater than 1 cm but less than or equal to 2 cm, greater than 2 cm but less than or equal to 3 cm, and greater than 3 cm, respectively. Neurological death was defined as death due to any form of intracranial disease, including tumor recurrence, carcinomatous meningitis, cerebral dissemination, and other unrelated intracranial diseases, as described by Patchell, et al.[4] Impaired ADL function was defined as neurological status based on a KPS score of less than 70 (functional preservation), as reported by Aoyama and coworkers.[1]

Statistical Analysis

The intervals from the date of diagnosis of brain metastases at our center until the date of death (OS), neurological death (NS), impaired ADL (QS), and the appearance of new distant lesions (NLFS) were calculated using the Kaplan–Meier method. Tumor progression–free survival in all patients treated with GKS during the observation period was also analyzed. Prognostic values of the individual covariates for OS, NS, QS, and NLFS were obtained with the Cox proportional-hazards model. The following 12 dichotomized covariates were entered: age (< 65 years compared with ≥ 65 years); sex (male compared with female); extracranial lesion status (controlled compared with active); pretreatment KPS score (< 70 compared with ≥ 70); primary cancer organ (lung compared with nonlung); number of brain lesions (≤ four compared with > four); maximum lesion diameter (< 25 mm compared with ≥ 25 mm); initial total tumor volume (≤ 10 cm^3 compared with >10 cm^3); MR imaging findings of CSF dissemination (yes compared with no); chemotherapy (yes compared with no); craniotomy (yes compared with no); and time elapsed between diagnosis of primary cancer and brain metastases (synchronous compared with metachronous). A probability value of less than 0.001 was taken to represent a statistically significant difference.

Results

The distributions of patient characteristics and lesion types and locations are summarized in Table 1. The primary organs were the lung in 719 patients (69.8%), gastrointestinal in 124 (12.3%), breast in 68 (6.6%), urinary tract in 52 (5%), and others/undetermined in 67 (6.5%). The median number of lesions treated with the initial GKS was three (range one–25 lesions). During the follow-up period, the number of GKS procedures for new distant lesions averaged 1.8 ± 1.5, varying between one and 18, and the mean number of lesions treated with GKS per patient was 9.9 ± 16.6 (range one–109). In total, 1853 separate GKS procedures were required to treat 10, 163 lesions. The mean calculated tumor volume was 0.87 ± 2.64 cm^3 (median 0.08 cm^3; range 0.1–24 cm^3).

TABLE 1

*Dichotomized patient characteristics**

Characteristic	No. of Patients
age (yrs)	
<65	547
≥65	483
sex	
male	654
female	376
extracranial disease	
controlled	125
active	905
pretreatment KPS score	
<70	162
≥70	868
primary organ	
lung	719
nonlung	311
no. of lesions	
≤4	620 (single 276)
>4	410
max lesion size (mm)	
<25	675
≥25	355
total tumor vol (cm^3)	
≤10	757
>10	273
CSF dissemination	
yes	86
no	944
chemotherapy	
yes	409
no	621
craniotomy	
yes	145
no	885
metastasis	
synchronous	385
metachronous	645

The minimum dose to the tumor margin was 15 to 30 Gy (mean ± standard deviation 20.4 ± 2.0 Gy; median 20 Gy) with a 72.4% isodose contour (range 30–98%). The mean prescribed doses were 20.6 Gy in 8573 tiny, 20.3 Gy in 977 small, 19.2 Gy in 441 medium, and 15.7 Gy in 172 large lesions. Figure 1 shows the cumulative lesion progression-free survival curves stratified by lesion size. The tumor control rates at 1 year were 99.5% in tiny, 92.6% in small, 87.3% in medium, and 65.5% in large lesions. The differences were statistically significant ($p < 0.0001$). Among 184 lesions showing progression, we diagnosed tumor recurrence in 83 and radiation injury in 101. The median OS period was 8.6 months. In multivariate analysis, significant prognostic factors for OS were active extracranial disease ($p < 0.0001$, HR 4.184), low pretreatment KPS score ($p < 0.0001$; HR 2.050), and male sex ($p < 0.0001$; HR 1.561). The OS curves were compared by using the Radiation Therapy Oncology Group recursive partitioning analysis classes (Fig. 2). The neurological death–free rates were 89% at 1 year and 73.6% at 2 years. Among the 729 deaths, 125 (17.1%) were attributed to neurological death (NS). Causes of neurological death were carcinomatous meningitis in 54, recurrence of the treated lesion in 29, cerebral dissemination in 22, progression of an untreated lesion in 16, and other in four. The only significant poor prognostic factor for NS was carcinomatous

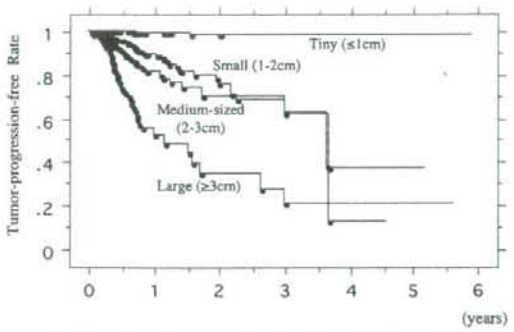

FIG. 1. Graph showing cumulative tumor progression–free survival curves, based on tumor size. The maximum lesion diameters are provided. The mean prescribed doses were 20.6 Gy in 8573 tiny, 20.3 Gy in 977 small, 19.2 Gy in 441 medium, and 15.7 Gy in 172 large lesions. The tumor control rates at 1 year were 99.5% in tiny, 92.6% in small, 87.3% in medium, and 65.5% in large lesions. Differences were statistically significant ($p < 0.0001$).

meningitis ($p < 0.0001$, HR 4.841). The NS curves were compared between patients with and without MR imaging findings of carcinomatous meningitis (Fig. 3). The QS rates were 82.1% at 1 year and 62.9% at 2 years. The MR imaging findings of CSF dissemination ($p < 0.0001$; HR 3.305) and active extracranial disease ($p < 0.0001$; HR 2.237) were confirmed to be significant factors influencing QS. No patient suffered radiation-induced dementia in this study. The NLFS rate at 1 year was 49.3%. According to multivariate analysis, the significant poor prognostic factors for NLFS were more than four brain metastases and active extracranial disease (Table 2). The NLFS curves based on tumor number are shown in Fig. 4. Among the 729 patients who died, the number of salvage GKS treatments for new distant lesions was zero in 470, one in 134, two in 62, three in 26, and more than four in 37. Salvage WBRT was subsequently performed in 30 patients with cerebral dissemination or CSF dissemination, which had been uncontrolled after aggressive GKS salvage treatment.

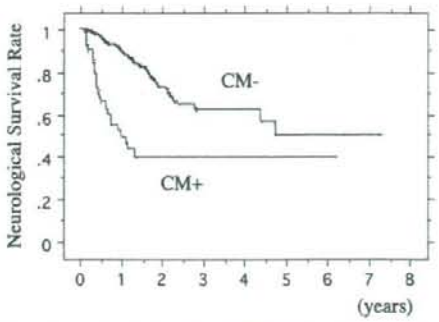

FIG. 3. Graph showing NS curves for patients with and without MR imaging evidence of carcinomatous meningitis. The neurological death–free rates at 1 year were 90.2% in patients with carcinomatous meningitis and 52.4% in those without. The difference was statistically significant ($p < 0.0001$). CM = carcinomatous meningitis.

Discussion

A few retrospective, randomized, controlled studies in which radiosurgery and radiosurgery plus initial adjuvant WBRT were compared have been reported.[1–3,9,10] In the Japanese Radiation Oncology Study Group series reported on by Aoyama, et al.,[1] no significant differences were found in OS, NS, or QS between radiosurgery alone and radiosurgery after adjuvant WBRT, although new lesions were observed more frequently with radiosurgery alone. These results support our treatment protocol of using GKS aggressively, at least in patients with only a few metastases. Our study comprised a very large series of patients who underwent GKS and did not receive any initial adjuvant WBRT. All patients were treated using the same treatment protocol. We have carefully analyzed the results and focused particular attention on new distant lesions.

New Distant Lesions and Salvage Treatment

Since the advent of computed tomography scanning, it has come to be widely believed that even patients with only a single metastatic lesion harbor microscopic

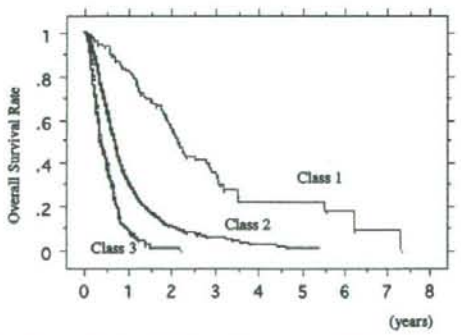

FIG. 2. Graph showing the OS curves stratified by Radiation Therapy Oncology Group recursive partitioning analysis classes. The median OS period was 2.2 years in Class 1, 0.71 years in Class 2, and 0.39 years in Class 3. Differences among the three classes were statistically significant ($p < 0.0001$).

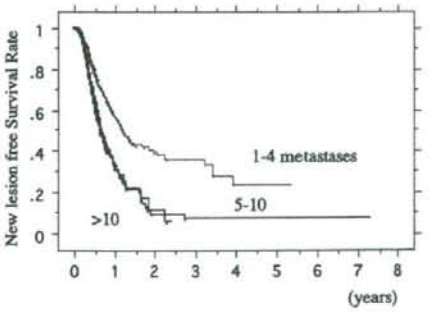

FIG. 4. Graph showing the NLFS curves based on tumor number. The new lesion–free rates at 1 year were 57.2% in patients with one to four brain metastases, 34.2% in those with five to 10, and 32.9% in those with more than 10. The difference between one to four and more than four brain metastases was statistically significant ($p < 0.0001$).

TABLE 2
Prognostic variables for NLFS

Variable	High Risk Group	p Value*	HR*	p Value†	HR†
age	<65	0.0441	1.229		
sex	male	0.4949	1.073		
extracranial disease	active	<0.0001	1.835	0.0005	1.656
initial KPS score	≥70	0.3603	1.161		
primary site	lung	0.9933	1.001		
no. of lesions	>4	<0.0001	1.844	<0.0001	1.734
max lesion size	<25 mm	0.9394	1.016		
total tumor vol	>10 cm^3	0.0826	1.316		
CSF dissemination	no	0.3327	1.232		
chemotherapy	yes	0.5884	1.057		
craniotomy	no	0.7755	1.038		
metastasis	synchronous	0.6298	1.052		

*Values are based on univariate analysis.
†Values are based on multivariate analysis (Cox proportional-hazards model).

metastases.[2,3] Modern high-resolution MR imaging can detect tumors only a few millimeters in diameter, and even these tiny metastatic lesions can be safely and accurately treated with GKS. The patient survival period may be too short for invisible metastases or true new lesions to be identified on follow-up MR imaging or to cause neurological symptoms. Chemotherapy may, of course, play an additional role in controlling microscopic lesions, especially in cancers sensitive to chemotherapy, such as small cell lung cancer and breast cancer. Our experience suggests that local control is the most important clinical goal for patients with brain metastases and that it is not necessary to treat invisible metastases. Indeed, approximately two-thirds of patients in this series did not require salvage treatment. If new lesions are detected, appropriate salvage treatment, taking patient condition into consideration, may be warranted. Whole-brain radiotherapy should be used only with great caution because of its invasive nature. The current study demonstrates that a local GKS treatment protocol without upfront WBRT can provide highly satisfactory results in selected patients.

Cost of GKS Alone Protocol

The cost of any local treatment protocol, without prophylactic WBRT, must always be considered. In Japan, GKS is relatively inexpensive, approximately 4000 US dollars; WBRT is less expensive and costs closer to 2500 US dollars. In this series, the mean number of GKS salvage treatments for new distant lesions was 0.8 per patient. The incidence of new distant lesions that can be controlled using GKS is expected to be 50%, provided all invisible microscopic lesions are controlled by initial WBRT. Thus, the total treatment costs come to approximately 7200 US dollars for GKS without prophylactic WBRT ($4000 + 4000 \times 0.8$) and 8100 US dollars for GKS with prophylactic WBRT ($4000 + 2500 + 4000 \times 0.4$). This local treatment is thus estimated to be less expensive than GKS with initial WBRT, although some patients may require frequent salvage GKS. The Japanese public insurance system covers all initial and salvage GKS procedures as well as follow-up MR imaging. Economic factors impacting radiosurgery and radiotherapy apparently differ markedly among countries. If the portions of fees for radiosurgery and radiotherapy covered by health insurance are similar to those in Japan, the cost of our local treatment protocol without prophylactic WBRT would appear to be quite reasonable.

Indications for and Limitations of our Local Treatment Protocol

Factors that limit the performance of single-session GKS include not only the number but also the size of lesions. Earlier reviews focused solely on number of lesions. To resolve this problem, we have proposed the TSID concept, which provides information on the limitations of safe GKS in a single session.[5–7] A TSID of 10 J is equivalent to 3 Gy of whole-skull radiation or a total tumor volume of 15 cm^3. This is also the WBRT single-fraction dose used for metastatic brain tumors (30 Gy in 10 fractions). If the lesions are scattered diffusely and similar of size, 25 tiny, 10 small, or four medium lesions would be the treatment limits of a single GKS session, assuming the peripheral doses are all 20 Gy. Adverse early radiation effects such as acute brain swelling were not observed in the present series with the TSID below 10 J. Yamamoto and colleagues[11] and Yang and coworkers,[12] although using higher radiation doses than allowed by our criteria, reported the safety of GKS for numerous brain metastases. The present criteria exclude patients with symptomatic carcinomatous meningitis, but thin-slice MR imaging for dose planning revealed asymptomatic CSF dissemination to be a highly significant poor prognostic factor for NS and QS. Thus, the exclusion criteria for this treatment are any surgically inaccessible huge (≥ 35 mm) tumor; tumor number and size exceeding a TSID of 10 J; and MR imaging findings of CSF dissemination. More than four brain metastases and active extracranial lesions were recognized as poor prognostic factors for new distant lesions on multivariate analysis. However, having more than four metastases did not affect OS, NS, or QS on multivariate analysis. For patients with more than four metastases, a randomized controlled study in which GKS alone is compared with GKS plus initial adjuvant WBRT should be performed.

Conclusions

In terms of NS and QS, GKS without initial adjuvant WBRT for brain metastases from various primary cancers provides excellent palliation considering the patients' short life expectancies. New distant lesions were fairly

well controlled with GKS salvage treatment alone, even in patients with more than four brain metastases; however, careful observation with enhanced MR imaging at intervals of no more than 3 months is necessary.

References

1. Aoyama H, Shirato H, Tago M, Nakagawara K, Toyoda T, Hatano K, et al: Stereotactic radiosurgery plus whole brain radiation therapy vs stereotactcic radiosurgery alone for treatment of brain metastases: a randomized controlled trial. **JAMA 295:**2483–2491, 2006
2. Arriagada R, Le Chevalier T, Borie F, Riviere A, Chomy P, Monnet I, et al: Prophylactic cranial irradiation for patients with small-cell lung cancer in complete remission. **J Nat Cancer Inst 87:**183–190, 1995
3. Kondziolka D, Patel A, Lunsford LD, Kassam A, Flickinger JC: Stereotactic radiosurgery plus whole brain radiotherapy versus radiotherapy alone for patients with multiple brain metastases. **Int J Radiat Oncol Biol Phys 45:**427–737, 1999
4. Patchell RA, Tibbs PA, Walsh JW, Dempsey RJ, Maruyama Y, Kryscio RJ, et al: A randomized trial of surgery in the treatment of single metastases to the brain. **N Engl J Med 322:**494–500, 1990
5. Serizawa T, Iuchi T, Ono J, Saeki N, Osato K, Odaki M, et al: Gamma Knife treatment for multiple metastatic brain tumors compared with whole-brain radiation therapy. **J Neurosurg (Suppl 3) 93:**32–36, 2000
6. Serizawa T, Ono J, Iuchi T, Matsuda S, Sato M, Odaki M, et al: Gamma Knife radiosurgery for metastatic brain tumors from lung cancer. Comparison between small cell cancer and non-small cell cancer. **J Neurosurg (Suppl 5) 97:**484–488, 2002
7. Serizawa T, Saeki N, Higuchi Y, Ono J, Iuchi T, Nagano O, et al: Gamma Knife surgery for brain metastases: indications for and limitations of a local treatment protocol. **Acta Neurochir (Wien) 147:**721–726, 2005
8. Serizawa T, Saeki N, Higuchi Y, Ono J, Matsuda S, Sato M, et al: Diagnostic value of thallium-201 chloride single-photon emission computed tomography in differentiating tumor recurrence from radiation injury after Gamma Knife surgery for metastatic brain tumors. **J Neurosurg (Suppl 2) 102:** 266–271, 2005
9. Sneed PK, Lamborn KR, Forstner JM, McDermott MW, Chang S, Park E, et al: Radiosurgery for brain metastases: is whole brain radiotherapy necessary? **Int J Radiat Oncol Biol Phys 43:**549–558, 1999
10. Sneed PK, Suh JH, Goetsch SJ, Sanghavi SN, Chappell R, Buatti JM, et al: A multi-institutional review of radiosurgery alone vs. radiosurgery with whole brain radiotherapy as the initial management of brain metastases. **Int J Radiat Oncol Biol Phys 53:**519–526, 2002
11. Yamamoto M, Ide M, Nishio S, Urakawa Y: Gamma Knife radiosurgery for numerous brain metastases: Is this a safe treatment? **Int J Radiat Oncol Biol Phys 53:**1279–1283, 2002
12. Yang CC, Ting J, Wu X, Markoe A: Dose volume histogram analysis of Gamma Knife radiosurgery treating twenty-five metastatic intracranial tumors. **Stereotac Funct Neurosurg 70:**41–49, 1998

Address reprint requests to: Toru Serizawa, M.D., Ph.D., Department of Neurosurgery, Chiba Cardiovascular Center, 575 Tsurumai, Ichihara, Chiba, 2900512 Japan. email: gamma-knife.serizawa@nifty.com.

J Neurosurg 104:598–607, 2006

Dissociated expressive and receptive language functions on magnetoencephalography, functional magnetic resonance imaging, and amobarbital studies

Case report and review of the literature

KYOUSUKE KAMADA, M.D., FUMIYA TAKEUCHI, M.D., SHINYA KURIKI, M.D., TOMOKI TODO, M.D., AKIO MORITA, M.D., AND YUTAKA SAWAMURA, M.D.

Department of Neurosurgery, Faculty of Medicine, The University of Tokyo; and Department of Neurosurgery and Research Institute for Electronic Science, Hokkaido University, Sapporo, Japan

Dissociated language functions are largely invalidated by standard techniques such as the amobarbital test and cortical stimulation. Language studies in which magnetoencephalography (MEG) and functional magnetic resonance (fMR) imaging are used to record data while the patient performs lexicosemantic tasks have enabled researchers to perform independent brain mapping for temporal and frontal language functions (MEG is used for temporal and fMR imaging for frontal functions). In this case report, the authors describe a right-handed patient in whom a right-sided insular glioma was diagnosed. The patient had a right-lateralized receptive language area, but expressive language function was identified in the left hemisphere on fMR imaging– and MEG-based mapping. Examinations were performed in 20 right-handed patients with low-grade gliomas (control group) for careful comparison with and interpretation of this patient's results. In these tests, all patients were asked to generate verbs related to acoustically presented nouns (verb generation) for fMR imaging, and to categorize as abstract or concrete a set of visually presented words consisting of three Japanese letters for fMR imaging and MEG.

The most prominent display of fMR imaging activation by the verb-generation task was observed in the left inferior and middle frontal gyri in all participants, including the patient presented here. Estimated dipoles identified with the abstract/concrete categorization task were concentrated in the superior temporal and supramarginal gyri in the left hemisphere in all control patients. In this patient, however, the right superior temporal region demonstrated significantly stronger activations on MEG and fMR imaging with the abstract/concrete categorization task. Suspected dissociation of the language functions was successfully mapped with these two imaging modalities and was validated by the modified amobarbital test and the postoperative neurological status. The authors describe detailed functional profiles obtained in this patient and review the cases of four previously described patients in whom dissociated language functions were found.

KEY WORDS • amobarbital test • functional magnetic resonance imaging • magnetoencephalography • language mapping • language function

BRAIN asymmetries have been of considerable interest in the field of neurology for more than a century. A classic mode of language organization based on lesional studies proposes a frontal expressive area, named for Broca, for planning and executing speech and writing, and a posterior receptive area, named for Wernicke, for analysis and identification of linguistic sensory stimuli. This basic scheme of language function has been generally accepted, with the assumption that both of the classic language functions exist only in the dominant hemisphere.

The amobarbital test is currently used to determine language dominance, but requires catheterization of the carotid arteries and successive anesthetization of each hemisphere by unilateral injections of sodium amobarbital. Data from previous studies have indicated that among right-handed participants, 4% have speech dominance generally in the right hemisphere, and in 90% it is found in the left hemisphere.[3] Several studies in which this technique was used have shown an increased incidence of atypical language dominance patterns in patients with injury in the left hemisphere. These patterns have been interpreted in terms of

Abbreviations used in this paper: BVRT = Benton Visual Retention Test; fMR = functional magnetic resonance; ICA = internal carotid artery; IQ = intelligence quotient; MEG = magnetoencephalography; WAB = Western Aphasia Battery; WAIS-R = Wechsler Adult Intelligence Scale–Revised.

interhemispheral language transfer and cerebral plasticity.[6,20] The amobarbital test, however, measures only the relative distribution of language across the two hemispheres and is not usually repeatable. More specific information and careful interpretation between hemispheres are practically and scientifically important factors for understanding the language networks.

The recently developed fMR imaging modality has been used to identify the dominant hemisphere for language functions. Most fMR imaging studies of language location have shown frontal activation in the inferior and middle frontal gyri during performance of various tasks, such as verb (word) generation and word categorization.[15,22,27] Although several authors have attempted to detect the receptive language function with fMR imaging by using listening or sentence comprehension tasks, only a few pixels revealing activation have been observed in the temporoparietal region.[8,15,23,24] Therefore, empirical evidence has shown that temporal activation is more difficult to detect than frontal activation. In addition, a fundamental limitation of fMR imaging–based brain mapping involves the varying degrees of regional hemodynamic responses in pathological brain conditions.[7,9,14] Therefore, the interpretation of fMR imaging–based localization for receptive language function remains difficult and controversial.

The MEG modality reflects the intracellular flow of electrical current in the brain and allows accurate localization of the current's dipole sources. Regarding language function, Papanicolaou and colleagues[17,18] localized MEG deflections, which peaked at approximately 400 msec after word presentation (late responses), in the temporoparietal regions. These investigators suggested that the late responses were strongly related to receptive language function. We have also reported dense dipole clusters of the semantic late responses in the superior temporal, supramarginal, and fusiform gyri of the suspected dominant hemisphere.[11,12] Therefore, MEG is a powerful diagnostic tool for identifying language dominance and the Wernicke area.

Given these findings, we have used fMR imaging and MEG modalities to visualize the expressive and receptive language functions independently and to identify the dominant hemisphere. In this case report, we describe a right-handed patient who had a right-sided insular glioma and a confirmed right-lateralized receptive language area, but in whom dissociated expressive function was found in the left hemisphere. The suspected dissociation of language functions was clearly mapped with fMR imaging and MEG, and was validated by the amobarbital test and the patient's postoperative neurological status. We describe detailed neurological and radiological findings characterizing the unusual functional organization in this patient, comparing these with the fMR imaging–MEG templates obtained in 20 control patients who underwent imaging in our institution. We also discuss the data acquired in four previously reported patients with dissociated language functions on fMR imaging–based brain mapping.

Case Report

History. This 29-year-old, right-handed man experienced amnesia for several minutes in November 2003. He has suffered from depression for 10 years and has been unemployed, despite the absence of neurological deficits. Computerized tomography scanning of the brain performed 11 years earlier had revealed no abnormality. The patient has been treated with several of the most commonly used tranquilizers in the outpatient clinic of our Department of Psychiatry. Neuropsychological examinations, including the WAIS-R and the BVRT, which were performed in April 1992, demonstrated no language deficit or memory disturbance, and the patient had a full-scale IQ of 86 (Table 1).

Neuroimaging, Neuropsychological Evaluation, and Surgical Planning. In November 2003, T_1-weighted MR images revealed a hypointense mass in the right insular cortex involving the surrounding white matter. The lesion was homogeneously hyperintense on T_2-weighted MR images and was not enhanced by addition of Gd–diethylenetriamine pentaacetic acid (Fig. 1A). These findings suggested that a

TABLE 1

Sequential results of neuropsychological examinations in a patient with dissociated language function*

Test	Item	Date of Evaluation & Score		
		4/1/1992	11/2/2002 (preop)	3/3/2003 (postop)
WAIS-R	verbal IQ	95	98	90
	information	9	10	9
	digit span	8	9	8
	vocabulary	10	12	8
	arithmetic	6	6	6
	comprehension	12	12	8
	similarities	10	9	10
	performance IQ	76	75	74
	picture completion	8	7	8
	picture arrangement	11	8	8
	block design	6	8	5
	object assembly	7	9	8
	digit symbol	3	3	3
	full-scale IQ	186	87	82
BVRT	no. of errors (normal mean, 5)	2	5	7
WMT	memory quotient	93	101	105
WAB	aphasia quotient	NT	98.6	92.8

* NT = not tested; WMT = Wechsler memory test.

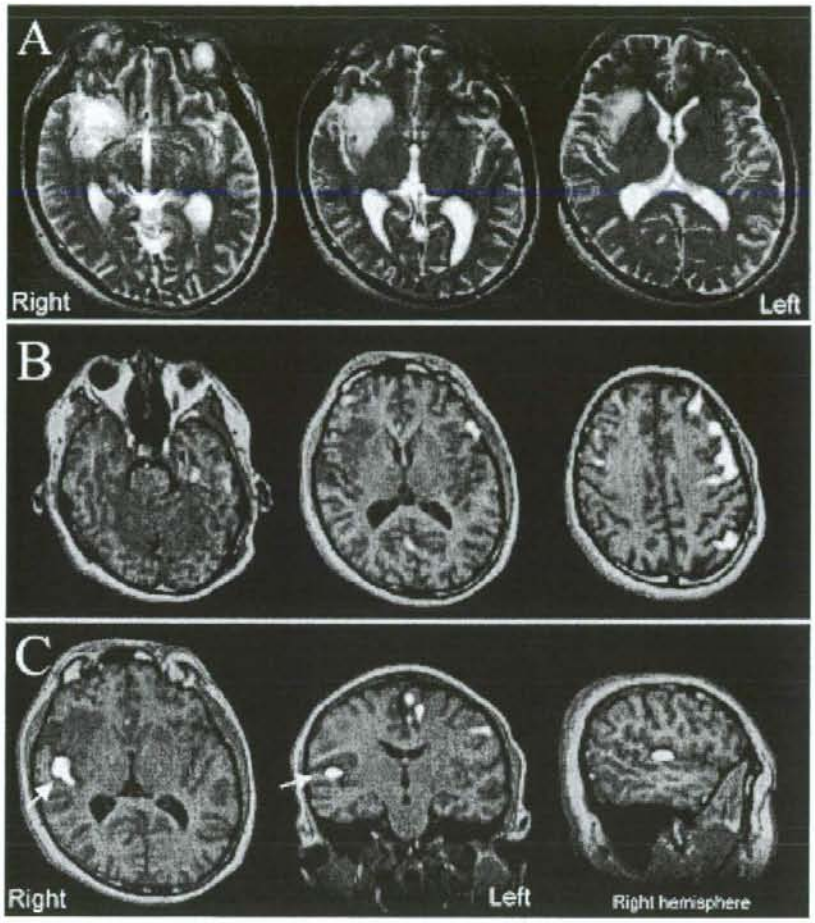

FIG. 1. A: Axial T_2-weighted MR images obtained in a 29-year-old man, demonstrating a right insular tumor. B: Brain activation measured using fMR imaging during the verb-generation task. The images display all activated areas with a Z-score of more than 2.2, which are mainly located in the inferior and middle frontal gyri. C: Activation on fMR images during the abstract/concrete categorization task, demonstrating right-sided dominance in the superior temporal region (arrows). The dissociated language function is observed in the left frontal and right temporal regions.

low-grade astrocytoma might have developed slowly over the past 11 years. The Edinburgh Handedness Inventory score was 114, indicating strong right-handed dominance. Preoperative neuropsychological examinations, including the WAB, in addition to the WAIS-R and BVRT, detected no language deficit or memory disturbance (Table 1). Performance IQ, verbal IQ, and memory function were unchanged from the previous examinations. Considering the tumor's location, the symptoms, and the patient's handedness, we planned to perform a radical resection.

Because we have previously reported elsewhere that postsurgical language deficits can be predicted based on results of MEG studies,[12] and have evaluated more than 70 patients by using both MEG and fMR imaging to identify the language dominance, this patient underwent functional brain mapping as usual. To obtain the standard language template for MEG- and fMR imaging–based brain mapping, we selected 20 control patients with low-grade gliomas (four tumors in the left frontal or right temporal lobe, and six in the left temporal or right frontal lobe). Eight gliomas involved the right and six involved the left insular region on T_2-weighted images. All patients in the control group had left-hemisphere language dominance, which was confirmed with the amobarbital test.

Protocols for MR Imaging. Anatomical MR and fMR imaging were performed during the same session with a 1.5-tesla whole-body MR unit equipped with echoplanar capabilities and a standard whole-head transmitter–receiver coil (Vision; Siemens, Erlangen, Germany). During the experiments, foam cushions were used to immobilize the patient's head.

Language Tasks Used for fMR Imaging. All language tasks that required responses were performed covertly. The fMR

images were acquired with a T_2-weighted echoplanar imaging sequence (TE 62 msec; TR 114 msec; flip angle 90°; slice thickness 4 mm; slice gap 2 mm; field of view 260 mm; matrix 64 × 128; 14 slices). Each fMR imaging session consisted of three dummy scan volumes, three activation periods, and four baseline (rest) periods. During each period, five echoplanar imaging volumes were collected, yielding a total of 38 imaging volumes. The fMR imaging data for language-related semantic responses were acquired as follows. All participants were examined using two different lexicosemantic language paradigms: 1) verb generation after acoustic presentation of nouns; and 2) abstract/concrete categorization of words after their presentation for reading. All words for semantic tasks were selected from common Japanese words listed in the electronic dictionary of the National Institute for Japanese Language.

Verb-Generation Task. For the verb-generation task, common concrete nouns were presented aurally. The auditory stimuli (duration range 400–600 msec) were produced by a native Japanese speaker with a flat intonation and were digitized, with a sampling rate of 44,000 Hz. Backward playback of the sound files was used to eliminate the primary auditory activation for the rest period with exactly the same interstimulus intervals (1600–2400 msec) as the active condition. The auditory stimuli were delivered binaurally through two 5-m-long plastic tubes terminating at a set of headphones. The sound intensity was an approximately 95-decibel sound pressure level at the participant's ear. Individuals were instructed to generate silently a verb related to each noun presented during the active periods.

Abstract/Concrete Categorization Task. Visual stimuli were presented on a liquid crystal display monitor, and a mirror positioned above the head coil allowed the patients to see the stimuli. During the abstract/concrete categorization task, words consisting of three kana letters (Japanese phonetic symbols) were presented with a 300-msec exposure time and an interstimulus interval ranging from 1800 to 2200 msec. Participants were instructed to categorize the presented word covertly as abstract or concrete. During the control period, they passively viewed random dots, which were created by destructuring kana letters and were controlled to have the same brightness as the kana words to eliminate primary visual responses. Before undergoing imaging studies, all participants had practiced briefly, and two fMR imaging examinations were performed for each task to confirm the consistency of results.

After data acquisition, a motion detection program (MEDx; Medical Numerics, Sterling, VA) discarded fMR sessions containing motion artifacts of more than 25% of the pixel size. After applying a gaussian spatial filter (7 mm in half width), functional activation maps were calculated by estimating Z-scores between the rest and activation periods with Dr. View software (Asahi Kasei, Tokyo, Japan). Clusters consisting of more than 10 pixels with a Z-score of higher than 2.2 were accepted as indicating real activation. The result of each fMR session was coregistered to three-dimensional T_1-weighted MR images of each participant's head, maximizing the mutual information of the data sets with the Affine transformation.[4,16]

Protocol for Lexicosemantic MEG. The MEG signals were recorded with a 204-channel biomagnetometer (Vector View; Neuromag, Helsinki, Finland) in a magnetically shielded room. We repeatedly acquired two data sets with each task to confirm stability and the MEG responses on two different days (10 and 7 days before the operation). One hundred fifty words were presented visually with a 300-msec exposure time, with interstimulus intervals ranging from 2800 to 3200 msec during MEG recordings. Each word consisted of three kana letters and was grammatically a noun. All patients were asked to categorize the presented word as abstract or concrete, pushing a button with the index finger for an abstract word or with the middle finger for a concrete one (kana-reading task). To identify the lexicosemantic responses specific to the kana-reading task, we presented 150 pairs of Arabic letters and asked patients to decide whether each pair had the same letters or different ones (figure-discrimination task). All patients participated in brief practice sessions before the measurement. Each epoch consisted of a 500-msec prestimulus baseline and a 1500-msec analysis period following stimulus delivery. The averaged magnetic signals were digitally filtered between 0.1 and 30 Hz. Significant MEG deflections were visually identified on the basis of the root mean squared fields of more than 10 sensors in the frontotemporal or temporooccipital regions. Locations and moments of equivalent current dipoles were calculated every 2 msec from 250 to 600 msec after the stimulus onsets by using the single equivalent dipole model. Only dipoles with a correlation value of more than 0.90 were accepted and were superimposed onto three-dimensional T_1-weighted MR images by identifying anatomical fiduciary landmarks. To confirm the calculated results, the same MEG time sections were analyzed with one of the current density maps; this is called the multiple current estimate.[26]

Protocol for the Amobarbital Test. All patients received injections of amobarbital (100 mg in a 10% solution) through the ICA. Language testing was performed during the initial period of maximal amobarbital action, which was indicated by contralateral brachial plegia. The following tasks were included: Task I, spontaneous counting (patients started counting just before amobarbital injection and were told to continue counting until the investigator presented the next task); Task II, letter reading (patients were then told to read aloud seven words consisting of three or four kana letters); Task III, naming (patients were asked to name aloud five objects that were pictorially presented); Task IV, auditory comprehension (patients were asked to perform three simple tasks such as blinking their eyes, opening their mouth, and raising their unparalyzed arm); and Task V, pointing to objects (a table with pictures of four objects was presented, and patients were told to select one picture by pointing—"where is the rabbit," "point to the cat," and so on). Performance in Tasks I and III was considered to reflect the patient's expressive linguistic capacities, whereas Tasks II, IV, and V were used to screen receptive language functions.

Data Obtained in Control Patients

Findings on fMR Images. The regions activated by the verb-generation task were restricted mostly to the left hemisphere. The activated regions involved the inferior frontal gyrus and the middle frontal gyrus, the lateral precentral gyrus, the supramarginal gyrus, and the supplementary motor area. Although several activations were found on the right side, in the right middle frontal and lateral precentral

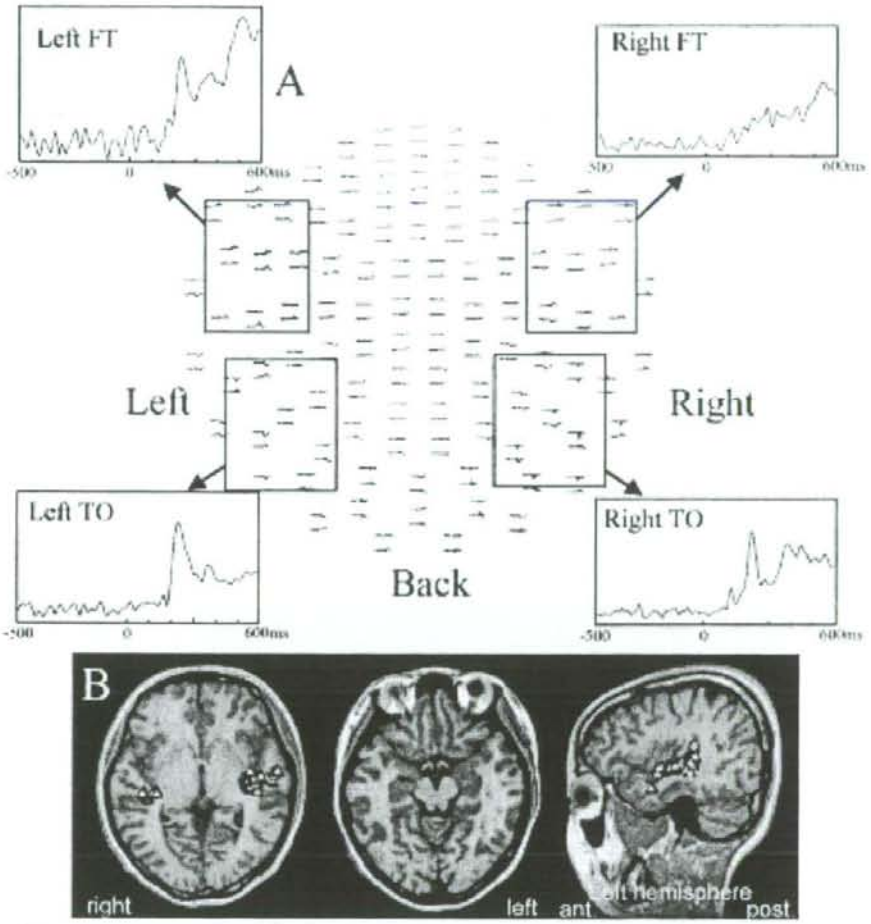

FIG. 2. A: Root mean squared profiles of lexicosemantic responses on both sides in the frontotemporal and temporooccipital regions on MEG studies obtained in a control patient. The left frontotemporal responses, peaking at 450 msec, are markedly larger in amplitude than the ones on the right. B: Neuroimages used in source localization of the late frontotemporal deflections, revealing predominant dipole clusters in the left superior temporal region. There are 107 dipoles in the left and 32 in the right hemisphere. FT = frontotemporal; ms = msec; TO = temporooccipital.

gyrus, they did not reach cluster significance (maximum values of Z-score < 2.2 or less than 10 pixels; data not shown). Although activations with the abstract/concrete categorization task tended to be lateralized to the left hemisphere, the bilateral frontal regions including the middle frontal and lateral precentral gyrus were involved. In addition, sporadically activated areas were found in the left superior temporal and the left fusiform gyri in seven of the 20 control patients.

The MEG Profiles and Dipole Locations. Figure 2 demonstrates results of imaging in a control patient. All patients were able to perform both tasks during data acquisitions. The values that follow are expressed as the means $\pm$ standard deviations. The mean reaction time and the rate of successful task performance in control patients were approximately 850.3 $\pm$ 32.4 msec and 94.2 $\pm$ 5.3%, respectively. In all control patients, the late deflections peaking at 400 msec were predominantly observed in the left rather than the right frontotemporal region (Fig. 2A). Bilateral temporooccipital regions demonstrated relatively early sharp deflections at approximately 250 msec with no hemispheral dominance in amplitude. As shown in Fig. 2B, the estimated dipoles of the frontotemporal regions were concentrated in the left superior temporal, middle temporal, and supramarginal gyri (the mean number of dipoles was 122.4 $\pm$ 24.2), whereas the right hemisphere showed far fewer dipoles (52.4 $\pm$ 14.2). In contrast, there were no significant hemispheral differences in the dipole concentration in the temporooccipital regions. Because the figure-discrimination task evoked only early deflections (within 300 msec) in both hemispheres with few late responses, on the basis of these results and previous reports, we speculate that late responses in the left hemisphere are strongly related to the lexicosemantic processes in letter perception.[11,12,18] In all control

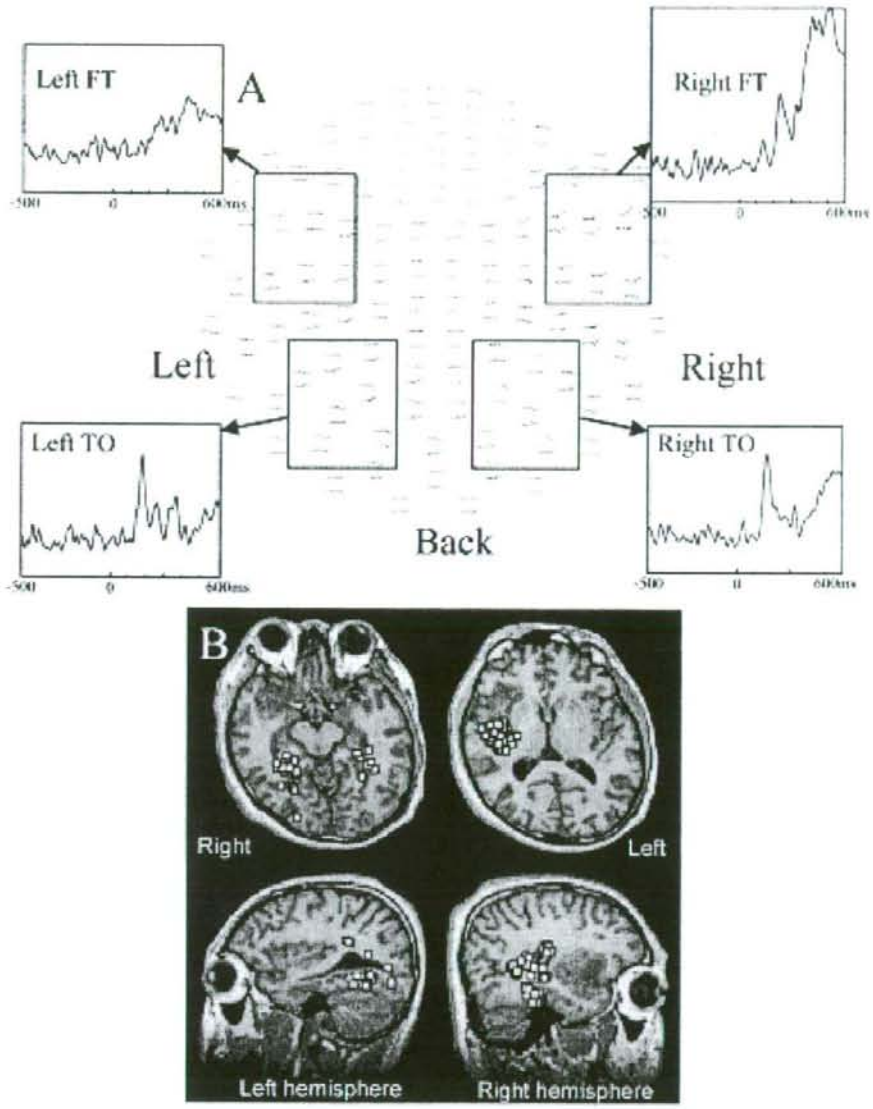

FIG. 3. A: Root mean squared profiles of lexicosemantic responses on both side in the frontotemporal and temporooccipital regions on MEG studies obtained in our patient. The right frontotemporal responses, peaking at 450 msec, are significantly larger in amplitude than the ones on the left. B: Neuroimages used in source localization of the late frontotemporal deflections, revealing predominant dipole clusters in the right superior and inferior temporal regions. There are 48 dipoles in the left and 202 in the right hemisphere.

patients, the activation profiles of fMR imaging and MEG studies clearly indicated left-sided dominance of the frontal expressive and temporal receptive language functions.

Data Obtained in Our Patient

Findings on fMR Images. The verb-generation task activated locations in our patient that were very similar to those in control patients. The left hemisphere had obvious activations in the inferior frontal, middle frontal, precentral, and supramarginal gyri, indicating that our patient had left-sided dominance of motor-language functions (Fig. 1B). In contrast, the abstract/concrete categorization task predominantly induced right-dominant activation in the temporal region, including the superior temporal and fusiform gyri (Fig. 1C). Based on these findings, we suggest that the language functions were separately distributed over both hemispheres.

TABLE 2
Results of the amobarbital test*

Item	Side of Test & Findings	
	Lt Injection	Rt Injection
paresis	rt hemi (4 mins)	lt hemi (4 mins, 30 secs)
counting	stopped (3 mins, 30 secs)	continued
letter-reading	71% (5 of 7)	14% (1 of 7)
naming	40% (2 of 5)	100% (5 of 5)
auditory comprehension	80% (4 of 5)	20% (1 of 5)
pointing to objects	100% (4 of 4)	25% (1 of 4)
general impression	impaired overt naming w/ severe dysarthria but little sensory aphasia	severe sensory aphasia w/ mild dysarthria

* Hemi = hemiparesis.

The expressive and receptive language functions were dissociated in the left frontal and right temporal lobes, respectively.

The MEG Profiles and Dipole Locations. The rate of successful task performance and the reaction time of the patient were within the control range. Figure 3A demonstrates the entire MEG view obtained in our patient, including the kana-reading task and the root mean squared fields in the bilateral frontotemporal and temporooccipital regions. Late deflections peaking at approximately 450 msec were more often observed in the right than in the contralateral frontotemporal region. There was no marked difference regarding side in the late responses in the temporooccipital regions. Estimated dipoles of the left frontotemporal responses were concentrated in the posterior part of the right superior temporal and middle temporal gyri (138 dipoles), which were adjacent to the posterior border of the tumor (Fig. 3B). In addition, another dipole cluster (64 dipoles) in the temporooccipital region was localized in the right fusiform gyrus. The total dipole number in the left hemisphere (48 dipoles) did not reach even a quarter of that in the right hemisphere, suggesting right-sided dominance of the reading process in this patient. The multiple current estimate analysis and the single equivalent dipole model demonstrated high current density spots in the posterior part of the right superior temporal and fusiform gyri. The figure-discrimination task evoked few late responses in either hemisphere. The second MEG performed on the 7th day before the operation yielded similar findings (right-sided dominance) in the temporoparietal regions.

A striking finding on the fMR imaging and MEG studies was that language functions in this patient might be dissociated over both hemispheres. We intended, therefore, to validate the neurological profiles with the amobarbital test before surgery.

The Amobarbital Test. The amobarbital test revealed left hemispheral dominance in all control patients, because the left ICA injection immediately disturbed all the motor and receptive-language functions.

Our patient stopped counting and failed to name objects (40%) after left ICA injection, whereas letter-reading (71%), auditory comprehension (80%), and pointing objects tasks (100%) were well preserved. In contrast, after right ICA injection, letter-reading (14%), auditory comprehension (20%), and pointing objects tasks (25%) were markedly suppressed, although the patient continued to count correctly without speech blockade (naming; 100%) but with slight hesitation. Detailed analysis of the results of the amobarbital test indicated interhemispheral dissociations of the expressive and receptive language functions (Table 2).

Operation. Although we obtained informed consent for radical resection of the tumor, the patient refused to undergo the awake surgical procedure. We therefore planned to perform tumor resection guided by the preoperative functional mapping. After integration of the lexicosemantic MEG dipoles into the neuronavigation system,[10] the insular cortex was exposed by a frontotemporal craniotomy. The tumor and involved brain tissue in the right anterior temporal and insular regions were removed in a gross-total fashion. We carefully spared suspected functional areas in the temporal lobe, where the MEG dipoles and the spots activated on fMR imaging were observed (Fig. 4). The histopathological diagnosis of this lesion was World Health Organization Grade II diffuse astrocytoma.

Postoperative Course. The patient awoke with slight, transient sensory aphasia after surgery. Although spontaneous speech and naming capacities were intact, mild sensory aphasia and dyslexia remained. Neuropsychological examinations conducted 4 months postsurgery disclosed slight impairment of vocabulary and comprehension, which resulted in deterioration of the patient's verbal IQ scores on the WAIS-R and the WAB tests (Table 1).

Discussion

The primary finding in this study was that the language dominance can be identified by combining different imaging methods. The use of fMR imaging with the verb-generation task detected the activation of the middle frontal and inferior frontal gyri, whereas MEG performed in conjunction with the kana-reading task localized the dipole clusters of the late responses in the superior temporal regions, such as the superior temporal and supramarginal gyri. These findings may mean that fMR imaging and MEG studies visualize independent centers for the expressive and receptive language functions in addition to indicating the language dominance. Particularly in our patient, fMR imaging and MEG studies demonstrated dissociated language functions over both hemispheres. The left frontal and right temporal regions took the expressive and receptive language roles, respectively. This unusual profile was consistently observed on repeated examinations and was finally validated by the results of the amobarbital test. After tumor resection, the patient experienced transient sensory aphasia for 1 week. Because the surgical procedure in the right frontotemporal region caused mild language deficits, the presence of aphasia supports the plausibility of the unusual functional profiles in this patient.

Kurthen, et al.,[13] first suggested the possibility of dissociated language functions when they used the amobarbital test to evaluate more than 100 patients with epilepsy. They reported on four patients with this disease who might have had independent frontal and temporal language centers in each hemisphere, and concluded that early-onset epilepsy might cause unusual representation of language functions. They did, however, find it difficult to distinguish the frontal

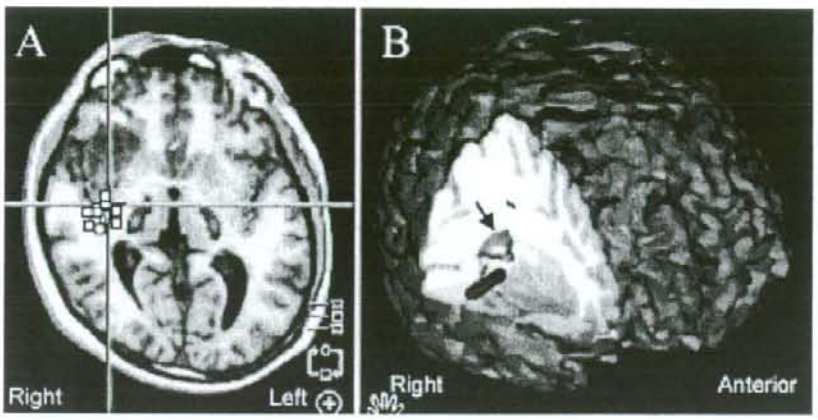

FIG. 4. A: Two-dimensional axial MR image demonstrating that the posterior border of resection is close to the dipole accumulation in the superior temporal region. B: Three-dimensionally reconstructed intracranial data obtained in our patient, clearly showing that a tip of the navigation probe (dark gray elongated oval) indicates the anterior border of lexicosemantic dipole clusters (arrow).

and temporal functions clearly because of the limited evaluation time associated with the amobarbital action and the level of patient cooperation. Noninvasive functional imaging techniques have recently become available to assess higher brain functions, and fMR imaging is becoming an alternative to the amobarbital test.[15,21,22] There have been few reports, however, of validations of the fMR imaging–activated areas by cortical stimulation.[22,24] It is still important to interpret fMR imaging results carefully by considering the results of the amobarbital test, electrocortical stimulation, and other functional imaging methods. Since the introduction of clinical fMR imaging, only four case reports have been published in which dissociated language functions were suggested (Table 3).[2,8,19,21]

Holodny, et al.,[8] and Baciu and colleagues[2] demonstrated translocation of the Broca area in isolation from temporal language function in patients with low-grade frontal glioma. Petrovich, et al.,[19] and Ries and coworkers[21] recently demonstrated that the temporal language function was translocated to the right hemisphere in patients with left temporal tumors. In their reports on fMR imaging, however, these investigators did not fully detail and confirm the unusual profiles with the amobarbital test. Using electrocortical stimulation, Baciu, et al., and Petrovich, et al., have observed no suppression of language function in frontal or temporal lobes containing tumors, findings that have caused them to stress the possibility of a functional dissociation.

Although fMR imaging–based brain mapping was used in all of these studies to investigate dissociation, in other reports researchers have found that even the various language tasks that are part of this modality produced little temporoparietal activation.[15,23,24] Rutten, et al.,[23,24] focused on the correspondence between fMR imaging and intraoperative electrocortical stimulation in the temporoparietal region. They applied several language tasks, such as picture naming, verbal fluency, and sentence comprehension, and concluded that much less activation appeared on fMR imaging in the temporoparietal than in the frontal area, but the physiological reason for this difference remains unknown. Because little neuronal activity is detected in the Wernicke areas on fMR imaging–based mapping, a more reliable method is required. One option that is highly complementary to fMR imaging is MEG. Simos and colleagues[25] have reported that the dipole localization of the lexicosemantic MEG in the temporoparietal region was reliable and showed excellent correlation with intraoperative cortical mapping. We believe that the combination of fMR imaging and MEG enables reliable identification of the expressive and receptive language functions.

In many previous reports, investigators have described either the shift or development of expressive and receptive language functions together in the expected nondominant right hemisphere.[1,5] Assuming that the dissociated language centers in our patient might reflect actual functional distributions, we must carefully consider the subcortical connections between the centers. Expressive and receptive language areas are usually connected by a large white-matter tract called the arcuate fasciculus. An arrangement in which the two language centers are in opposite hemispheres makes little physiological sense because it would involve a much more circuitous path of interaction between the centers. Recently developed diffusion tensor imaging might be used to clarify white-matter connections, such as the corpus callosum and the corticospinal tract. This technique, however, still has insufficient spatial resolution for small axonal bundles, including the anterior and posterior commissures. Although detailed physiological connections are still unclear, the technical development of diffusion tensor imaging might help resolve these issues in the near future.

Conclusions

Bilateral language dominance, which was generally determined with the amobarbital test, may involve dissociated frontal and temporal language functions. A slow-growing brain tumor or early-onset epilepsy might induce this unusual functional distribution. In our patient there remains speculation that the growth of the brain tumor prevented the

TABLE 3
Literature review of reports of dissociated language function*

Authors & Year	Patient: Age (yrs), Sex; Hand	Patient: Symptoms & Duration (yrs)	Tumor Location	Dominance on fMRI: Frontal	Dominance on fMRI: Temporal	Amobarbital Test: Expressive	Amobarbital Test: Receptive	Dominance on MEG (reading task)	Cortical Stimulation & Effect	Postop Course
Holodny, et al., 2002	34, M; rt	mild rt hemi, dysarthria (7)	lt insular (astrocytoma)	rt	lt	ND	ND	ND	ND	improved
Baciu, et al., 2003	30, M; lt	epilepsy, apraxia (26)	lt frontal (ganglioglioma)	rt	lt	failed†	failed†	ND	lt frontal (none)	no change
Petrovich, et al., 2004	62, M; rt	none	lt temporoparietal (astrocytoma)	lt	rt	ND	ND	ND	lt frontal (arrest); lt temporal (none)	improved
Ries, et al., 2004	13, F; ambi	epilepsy (10)	lt temporal (subependymoma)	lt	rt	rt	rt	ND	ND	improved
present study	29, M; rt	transient amnesia (–11)	rt insular (astrocytoma)	lt	rt	lt	rt	rt	ND	mild sensory aphasia

* Ambi = ambidextrous; hand = handedness; ND = not done.
† The amobarbital test failed to show dominance.

involved area from functioning properly and led to transfer of the expressive language function to the contralateral (left) side. On the other hand, this unusual functional organization may have been congenital. The reason for the dissociation, however, cannot be definitively determined. Based on our findings in this case, we would like to stress that the combination of fMR imaging and MEG studies can be used to identify functional characteristics in individual patients.

References

1. Abo M, Senoo A, Watanabe S, Miyano S, Doseki K, Sasaki N, et al: Language-related brain function during word repetition in post-stroke aphasics. Neuroreport 15:1891–1894, 2004
2. Baciu MV, Watson JM, McDermott KB, Wetzel RD, Attarian H, Moran CJ, et al: Functional MRI reveals an interhemispheric dissociation of frontal and temporal language regions in a patient with focal epilepsy. Epilepsy Behav 4:776–780, 2003
3. Branch C, Milner B, Rasmussen T: Intracarotid sodium amytal for the lateralization of cerebral speech dominance; observations in 123 patients. J Neurosurg 21:399–405, 1964
4. Chen HM, Varshney PK: Mutual information-based CT-MR brain image registration using generalized partial volume joint histogram estimation. IEEE Trans Med Imaging 22:1111–1119, 2003
5. Fernandez B, Cardebat D, Demonet JF, Joseph PA, Mazaux JM, Barat M, et al: Functional MRI follow-up study of language processes in healthy subjects and during recovery in a case of aphasia. Stroke 35:2171–2176, 2004
6. Helmstaedter C, Kurthen M, Linke DB, Elger CE: Patterns of language dominance in focal left and right hemisphere epilepsies: relation to MRI findings, EEG, sex, and age at onset of epilepsy. Brain Cogn 33:135–150, 1997
7. Holodny AI, Schulder M, Liu WC, Maldjian JA, Kalnin AJ: Decreased BOLD functional MR activation of the motor and sensory cortices adjacent to a glioblastoma multiforme: implications for image-guided neurosurgery. AJNR 20:609–612, 1999
8. Holodny AI, Schulder M, Ybasco A, Liu WC: Translocation of Broca's area to the contralateral hemisphere as the result of the growth of a left inferior frontal glioma. J Comput Assist Tomogr 26:941–943, 2002
9. Kamada K, Houkin K, Iwasaki Y, Takeuchi F, Kuriki S, Mitsumori K, et al: Rapid identification of the primary motor area by using magnetic resonance axonography. J Neurosurg 97: 558–567, 2002
10. Kamada K, Houkin K, Takeuchi F, Ishii N, Ikeda J, Sawamura Y, et al: Visualization of the eloquent motor system by integration of MEG, functional, and anisotropic diffusion-weighted MRI in functional neuronavigation. Surg Neurol 59:352–362, 2003
11. Kamada K, Kober H, Saguer M, Moller M, Kaltenhauser M, Vieth J: Responses to silent Kanji reading of the native Japanese and German in task subtraction magnetoencephalography. Brain Res Cogn Brain Res 7:89–98, 1998
12. Kamada K, Sawamura Y, Takeuchi F, Houkin K, Kawaguchi H, Iwasaki Y, et al: Gradual recovery from dyslexia and related serial magnetoencephalographic changes in the lexicosemantic centers after resection of a mesial temporal astrocytoma. Case report. J Neurosurg 100:1101–1106, 2004
13. Kurthen M, Helmstaedter C, Linke DB, Solymosi L, Elger CE, Schramm J: Interhemispheric dissociation of expressive and receptive language functions in patients with complex-partial seizures: an amobarbital study. Brain Lang 43:694–712, 1992
14. Lehericy S, Biondi A, Sourour N, Vlaicu M, du Montcel ST, Cohen L, et al: Arteriovenous brain malformations: is functional MR imaging reliable for studying language reorganization in patients? Initial observations. Radiology 223:672–682, 2002
15. Lehericy S, Cohen L, Bazin B, Samson S, Giacomini E, Rougetet

R, et al: Functional MR evaluation of temporal and frontal language dominance compared with the Wada test. Neurology 54: 1625–1633, 2000
16. Masutani Y, Aoki S, Abe O, Hayashi N, Otomo K: MR diffusion tensor imaging: recent advance and new techniques for diffusion tensor visualization. Eur J Radiol 46:53–66, 2003
17. Papanicolaou AC, Simos PG, Breier JI, Zouridakis G, Willmore LJ, Wheless JW, et al: Magnetoencephalographic mapping of the language-specific cortex. J Neurosurg 90:85–93, 1999
18. Papanicolaou AC, Simos PG, Castillo EM, Breier JI, Sarkari S, Pataraia E, et al: Magnetocephalography: a noninvasive alternative to the Wada procedure. J Neurosurg 100:867–876, 2004
19. Petrovich NM, Holodny AI, Brennan CW, Gutin PH: Isolated translocation of Wernicke's area to the right hemisphere in a 62-year-man with a temporo-parietal glioma. AJNR 25:130–133, 2004
20. Rasmussen T, Milner B: The role of early left-brain injury in determining lateralization of cerebral speech functions. Ann N Y Acad Sci 299:355–369, 1977
21. Ries ML, Boop FA, Griebel ML, Zou P, Phillips NS, Johnson SC, et al: Functional MRI and Wada determination of language lateralization: a case of crossed dominance. Epilepsia 45:85–89, 2004
22. Roux FE, Boulanouar K, Lotterie JA, Mejdoubi M, LeSage JP, Berry I: Language functional magnetic resonance imaging in preoperative assessment of language areas: correlation with direct cortical stimulation. Neurosurgery 52:1335–1347, 2003
23. Rutten GJ, Ramsey NF, van Rijen PC, Alpherts WC, van Veelen CW: FMRI-determined language lateralization in patients with unilateral or mixed language dominance according to the Wada test. Neuroimage 17:447–460, 2002
24. Rutten GJ, Ramsey NF, van Rijen PC, Noordmans HJ, van Veelen CW: Development of a functional magnetic resonance imaging protocol for intraoperative localization of critical temporoparietal language areas. Ann Neurol 51:350–360, 2002
25. Simos PG, Papanicolaou AC, Breier JI, Wheless JW, Constantinou JE, Gormley WB, et al: Localization of language-specific cortex by using magnetic source imaging and electrical stimulation mapping. J Neurosurg 91:787–796, 1999
26. Stenbacka L, Vanni S, Uutela K, Hari R: Comparison of minimum current estimate and dipole modeling in the analysis of simulated activity in the human visual cortices. Neuroimage 16:936–943, 2002
27. Yetkin FZ, Mueller WM, Morris GL, McAuliffe TL, Ulmer JL, Cox RW, et al: Functional MR activation correlated with intraoperative cortical mapping. AJNR 18:1311–1315, 1997

Manuscript received March 25, 2005.
Accepted in final form October 7, 2005.
This work was supported in part by the Japan Epilepsy Research Foundation; Takeda Promotion of Science Foundation; Grant-in-Aid No. 17591502 for scientific research from the Ministry of Education, Culture, Sports, Science and Technology; and a Research Grant from the Princess Takamatsu Cancer Research Fund.

Address reprint requests to: Kyousuke Kamada, M.D., Department of Neurosurgery, Faculty of Medicine, The University of Tokyo, Bunkyo-ku, Hongo 7-3-1, Tokyo 113-8655, Japan. email: kamady-k@umin.ac.jp.

Stereotactic Radiosurgery Plus Whole-Brain Radiation Therapy vs Stereotactic Radiosurgery Alone for Treatment of Brain Metastases

A Randomized Controlled Trial

Hidefumi Aoyama, MD, PhD
Hiroki Shirato, MD, PhD
Masao Tago, MD, PhD
Keiichi Nakagawa, MD, PhD
Tatsuya Toyoda, MD, PhD
Kazuo Hatano, MD, PhD
Masahiro Kenjyo, MD, PhD
Natsuo Oya, MD, PhD
Saeko Hirota, MD, PhD
Hiroki Shioura, MD, PhD
Etsuo Kunieda, MD, PhD
Taisuke Inomata, MD, PhD
Kazushige Hayakawa, MD, PhD
Norio Katoh, MD
Gen Kobashi, MD, PhD

Context In patients with brain metastases, it is unclear whether adding up-front whole-brain radiation therapy (WBRT) to stereotactic radiosurgery (SRS) has beneficial effects on mortality or neurologic function compared with SRS alone.

Objective To determine if WBRT combined with SRS results in improvements in survival, brain tumor control, functional preservation rate, and frequency of neurologic death.

Design, Setting, and Patients Randomized controlled trial of 132 patients with 1 to 4 brain metastases, each less than 3 cm in diameter, enrolled at 11 hospitals in Japan between October 1999 and December 2003.

Interventions Patients were randomly assigned to receive WBRT plus SRS (65 patients) or SRS alone (67 patients).

Main Outcome Measures The primary end point was overall survival; secondary end points were brain tumor recurrence, salvage brain treatment, functional preservation, toxic effects of radiation, and cause of death.

Results The median survival time and the 1-year actuarial survival rate were 7.5 months and 38.5% (95% confidence interval, 26.7%-50.3%) in the WBRT + SRS group and 8.0 months and 28.4% (95% confidence interval, 17.6%-39.2%) for SRS alone ($P = .42$). The 12-month brain tumor recurrence rate was 46.8% in the WBRT + SRS group and 76.4% for SRS alone group ($P < .001$). Salvage brain treatment was less frequently required in the WBRT + SRS group (n = 10) than with SRS alone (n = 29) ($P < .001$). Death was attributed to neurologic causes in 22.8% of patients in the WBRT + SRS group and in 19.3% of those treated with SRS alone ($P = .64$). There were no significant differences in systemic and neurologic functional preservation and toxic effects of radiation.

Conclusions Compared with SRS alone, the use of WBRT plus SRS did not improve survival for patients with 1 to 4 brain metastases, but intracranial relapse occurred considerably more frequently in those who did not receive WBRT. Consequently, salvage treatment is frequently required when up-front WBRT is not used.

Trial Registration umin.ac.jp/ctr Identifier: C000000412

JAMA. 2006;295:2483-2491 www.jama.com

BRAIN METASTASES OCCUR IN 20% to 40% of all patients with cancer and are generally associated with a poor prognosis.[1,2] The most common route of metastatic dissemination resulting in brain metastases is hematogenous, and it is therefore presumed that the entire brain is "seeded" with micrometastatic disease, even when only a single intracranial lesion is detected. Consequently, whole-brain radiation therapy (WBRT) has been a mainstay of treatment.[1,2]

Recently, the assumption that the entire brain is seeded with micrometastases in all patients with overt brain metastases has been questioned, prompting

For editorial comment see p 2535.

Author Affiliations: Departments of Radiology (Drs Aoyama, Shirato, and Katoh) and Global Health and Epidemiology, Division of Preventive Medicine (Dr Kobashi), Hokkaido University Graduate School of Medicine, Sapporo, Japan; Department of Radiology, University of Tokyo Hospital, Tokyo, Japan (Drs Tago and Nakagawa); Department of Radiology, Kanto Medical Center NTT EC, Tokyo, Japan (Dr Toyoda); Department of Radiology, Chiba Cancer Center, Chiba, Japan (Dr Hatano); Department of Radiology, Hiroshima University School of Medicine, Hiroshima, Japan (Dr Kenjyo); Department of Radiology, Kyoto University School of Medicine, Kyoto, Japan (Dr Oya); Department of Radiology, Hyogo Medical Center for Adults, Akashi, Japan (Dr Hirota); Department of Radiology, Izumisano General Hospital, Izumisano, Japan (Dr Shioura); Department of Radiology, Keio University School of Medicine, Tokyo, Japan (Dr Kunieda); Department of Radiology, Osaka Medical College, Osaka, Japan (Dr Inomata); Department of Radiology, Kitazato Medical School, Sagamihara, Japan (Dr Hayakawa).
Corresponding Author: Hidefumi Aoyama, MD, PhD, Department of Radiology, Hokkaido University Graduate School of Medicine, North 15, West 7, Kita-ku, Sapporo 060-8638, Japan (h-aoyama@umin.ac.jp).

a contrarian philosophy that in some patients, the intracranial disease is truly limited—the so-called oligometastases situation. For patients who truly have limited intracranial disease, the potential exists that WBRT could be replaced by focal therapeutic options such as resection or stereotactic radiosurgery (SRS), which delivers high-dose, focal radiation.[1-4]

The adverse effects of WBRT require a further examination of its role. Acute adverse effects are generally limited in severity and duration; however, the long-term risks of serious and permanent toxic effects, including cognitive deterioration and cerebellar dysfunction, are poorly understood.[5,6] In the attempt to minimize potential long-term morbidity following WBRT, treatments initially relying on focal therapeutic options are being used with increasing frequency. Although there have been several retrospective reports,[7-14] only 1 prospective randomized study compared the outcome of conventional surgery alone and surgery followed by WBRT.[6] Sneed et al[7] collected raw data on 983 patients from 10 institutions and suggested that there was no survival difference between patients treated with SRS alone and those treated with WBRT plus SRS. Flickinger et al[8] reviewed 116 patients with solitary brain metastases who underwent SRS with or without fractionated large-field radiotherapy and found improved local control, but not improved survival, with the addition of fractionated large-field radiotherapy. Regine et al[9] suggested that SRS alone is associated with an increasingly significant risk of brain tumor recurrence and neurologic deficit with increasing survival time. Pirzkall et al[10] showed a trend for superior local control and survival when SRS was combined with WBRT in 236 patients with 311 brain metastases. Aoyama et al,[11] Chidel et al,[12] and Shirato et al[13] have all shown that omission of WBRT from initial management was not detrimental in terms of overall survival, but brain tumors recurred in more than 50% of patients treated in this manner. Patchell et al[6] have shown that patients with cancer and single metastases to the brain who receive treatment with surgical resection and postoperative WBRT have fewer recurrences of cancer in the brain and are less likely to die of neurologic causes than are similar patients treated with surgical resection alone.

Herein, we report the results of a prospective, multi-institutional, randomized controlled trial comparing WBRT plus SRS vs SRS alone for patients with limited (defined as ≤4) brain metastases. Through a literature search and examination of clinical trial registries, we confirmed that this is the first multi-institutional, prospective, randomized comparison of WBRT plus SRS vs SRS alone.

METHODS

Eligibility Criteria

Patients were eligible who were aged 18 years or older with 1 to 4 brain metastases, each with a maximum diameter of no more than 3 cm on contrast-enhanced magnetic resonance imaging (MRI) scans, derived from a histologically confirmed systemic cancer. Patients with metastases from small cell carcinoma, lymphoma, germinoma, and multiple myeloma were excluded. Eligible patients had a Karnofsky Performance Status (KPS) score of 70 or higher. The protocol was approved by the institutional review boards of Hokkaido University, Sapporo, Japan, and of 10 other institutions that participated in the trial through the Japanese Radiation Oncology Study Group (JROSG 99-1). Written informed consent was obtained from each patient before entry into the study.

Randomization and Treatment

Randomization was performed at the Hokkaido University Hospital Data Center. A permuted-blocks randomization algorithm was used with a block size of 4. A randomization sheet was created for each institution. After written informed consent was obtained, eligible patients were randomly assigned to receive either up-front WBRT combined with SRS or SRS without up-front WBRT. Prior to randomization, the patients were stratified based on number of brain metastases (single vs 2-4), extent of extracranial disease (active vs stable), and primary tumor site (lung vs other sites). Extracranial disease was considered to be stable when the tumor had been clinically controlled for 6 months or longer prior to the detection of brain metastases.

The WBRT dosage schedule was 30 Gy in 10 fractions over 2 to 2.5 weeks. The WBRT treatment visit proceeded to SRS when patients were assigned to the WBRT + SRS group. The SRS dose was prescribed to the tumor margin. Metastases with a maximum diameter of up to 2 cm were treated with doses of 22 to 25 Gy and those larger than 2 cm were treated with doses of 18 to 20 Gy. The dose was reduced by 30% when the treatment was combined with WBRT because the optimal combination of WBRT and SRS had not been studied in well-conducted, prospective, phase I dose escalation trials. In the 1990s, the Radiation Therapy Oncology Group (RTOG) initiated a phase I dose escalation trial of SRS alone in patients who had previously undergone radiation treatment.[14] This trial was stopped early without reaching the maximum tolerance dose, and tumor size–dependent dose recommendations for SRS alone were described. No phase I trial has ever tested the combination of WBRT and SRS doses. Therefore, there is no well-known or scientifically recommended dose for the combination of WBRT and SRS. There are clearly concerns that the combination could be potentially deleterious. Therefore, various studies have adopted different approaches for selection of the dose combinations to be tested. Several retrospective data suggested that the RTOG dose guidelines might be associated with a higher frequency of late radiation toxic effects when used with WBRT.[10,15] Our preexisting experience of SRS with a 30% reduced SRS dose

combined with WBRT indicated that there is not a significant difference in local tumor control (data not shown) compared with SRS with the dose suggested in the RTOG protocol. Therefore, we decided to use a 30% reduced SRS dose in the WBRT + SRS group in this study.

Follow-up Protocol

We performed clinical evaluations and MRI scans 1 and 3 months after treatment and every 3 months thereafter. In cases in which a recurrence was detected, further treatment was administered at the discretion of the attending physician. The size of the treated lesions was measured in 3 dimensions, and this size, the development of new brain metastases, and the development of leukoencephalopathy associated with radiological findings (according to the National Cancer Institute's Common Toxicity Criteria version 2.0[16]) were scored based on serial MRI scans. Local tumor progression was defined as a radiographic increase of 25% or more in the size of a metastatic lesion (bidimensional product). If an MRI result showed central or heterogeneous low intensity and if the lesion size decreased on serial studies, brain necrosis was scored; positron emission tomography or surgical resection was encouraged as appropriate to confirm MRI findings.

At each visit, functional status and neurologic toxic effects were scored. Systemic functional status was evaluated by using the KPS score. Neurologic function was evaluated according to the criteria listed in TABLE 1.[17] Neurosurgeons or radiation oncologists specializing in neuro-oncology measured the neurologic status as well as the KPS score at the clinic. We did not attempt to blind the investigators with regard to patients' treatment assignments. Systematic functional status and neurologic function were scored by the physicians who treated the patients. An acute toxic effect was identified as an event that arose within 90 days of the initiation of radiotherapy and a late toxic effect was considered as an event that occurred thereafter, according to the central nervous system toxicity criteria listed among the RTOG Late Radiation Morbidity Scoring Criteria.[18] For all patients who died, the cause of death was determined. The cause of death was determined by autopsy in 1 patient and by clinical evaluation based on the definition proposed by Patchell et al[6] in all other patients. Patients were considered to have died of neurologic causes if they had stable systemic disease and

Table 1. Baseline Characteristics*

Characteristics	WBRT + SRS (n = 65)	SRS Alone (n = 67)
Age at diagnosis, mean (range), y	62.5 (36-78)	62.1 (33-86)
<65	32 (49)	34 (51)
≥65	33 (51)	33 (49)
Men	46 (71)	53 (79)
No. of brain metastases		
1	31 (48)	33 (49)
2-4	34 (52)	34 (51)
Primary tumor site		
Breast	6 (9)	3 (4)
Lung	43 (66)	45 (67)
Colorectal	5 (8)	6 (9)
Kidney	5 (8)	5 (7)
Other	6 (9)	8 (12)
Primary tumor status		
Stable	30 (46)	33 (49)
Active	35 (54)	34 (51)
Extracranial metastases		
Stable	41 (63)	38 (57)
Active	24 (37)	29 (43)
RPA		
Class 1 (aged <65 years; no active extracranial disease)	11 (17)	8 (12)
Class 2 (aged ≥65 years; active extracranial disease)	54 (83)	59 (88)
Histological status		
Squamous cell	11 (17)	11 (16)
Adenocarcinoma	43 (66)	43 (64)
Large cell	2 (3)	4 (6)
Other	9 (14)	9 (13)
KPS score†		
70-80	31 (48)	23 (34)
90-100	34 (52)	44 (66)
Neurologic function		
No symptoms (grade 0)	38 (59)	47 (70)
Minor symptoms; fully active without assistance (grade 1)	12 (18)	13 (19)
Moderate symptoms; fully active but requires assistance (grade 2)	8 (12)	4 (6)
Moderate symptoms; less than fully active, requires assistance (grade 3)	7 (11)	3 (5)
Severe symptoms; totally inactive (grade 4)	0	0
Chemotherapy after brain treatment	18 (38)	19 (40)
Maximum diameter of brain metastases, cm		
Mean (SD)	1.53 (0.78)	1.42 (0.79)
Median (range)	1.40 (0.2-3.0)	1.30 (0.2-3.0)
SRS dose at the tumor margin, mean (SD), Gy	16.6 (3.6)	21.9 (2.7)

Abbreviations: KPS, Karnofsky Performance Status; RPA, recursive partition analysis; SRS, stereotactic radiosurgery; WBRT, whole-brain radiation therapy.
*Data are expressed as No. (%) of participants unless otherwise noted.
†A higher score indicates better performance.

progressive neurologic dysfunction. Patients with severe neurologic disability who died of intercurrent illness were also included among neurologic deaths, as were patients with both rapidly progressive systemic disease and advancing neurologic dysfunction, because these patients also represent brain treatment failures.

Figure 1. Flow of Study Participants

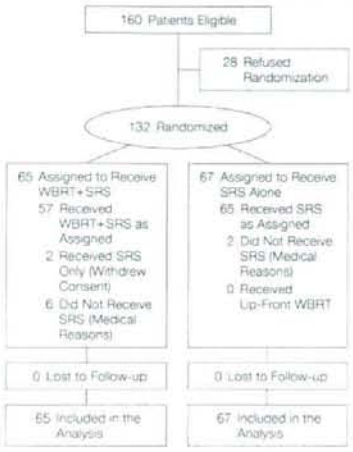

SRS indicates stereotactic radiosurgery; WBRT, whole-brain radiation therapy.

End Points and Statistical Analysis

The primary end point of the study was overall survival. Secondary end points were cause of death, functional preservation, brain tumor recurrence, salvage treatment, and toxic effects of radiation. All analyses were conducted on an intention-to-treat basis. The study was designed to have 80% power to detect an absolute difference of 30% in the median survival time, with a 2-sided α level of .05. Using an estimated median survival time of 8.7 months for the group receiving SRS alone[11] and a follow-up time of 15 months, the sample size required to detect this difference was 89 patients per group. An interim analysis was planned wherein 50 patients would be assigned to each group to determine whether the sample size was large enough to show a significant difference with a 2-sided α level of .05. End points were measured beginning at the date of randomization. Univariate analyses were carried out by the Kaplan-Meier method.[19] We assumed that the survival rate was always higher in the WBRT + SRS group than in the SRS-alone group based on the suggestions in a retrospective study, and we used the log-rank test to compare differences between the groups. The χ^2 test was used to determine the relationship between 2 categorical variables, and the Fisher exact test was used when small cell sizes were encountered in 2×2 contingency tables. A 2-tailed t test was used to compare the means of continuous variables between the treatment groups. Multivariate analyses were performed to evaluate the factors selected via the univariate analyses ($P<.10$). Stratification in the randomization was taken into account in the statistical analysis. The Cox proportional hazards model was used to calculate hazard ratios and 95% confidence intervals (CIs).[20] A 2-sided P value of .05 or less was considered to reflect statistical significance. Additional covariates were examined as appropriate and are noted in the "Results" section. All statistical analyses were initially performed by a physician (H.A.) using a commercial statistical software package (StatView version 5.0J, SAS Institute Inc, Cary, NC), and all results were verified by a statistician (G.K.) using a different software package (SAS, version 9.1, SAS Institute Japan Ltd, Tokyo, Japan).

RESULTS

Patients and Treatment

The recruitment period was from October 1999 to December 2003. There were

Figure 2. Overall Survival and Brain Tumor Recurrence at Distant Sites

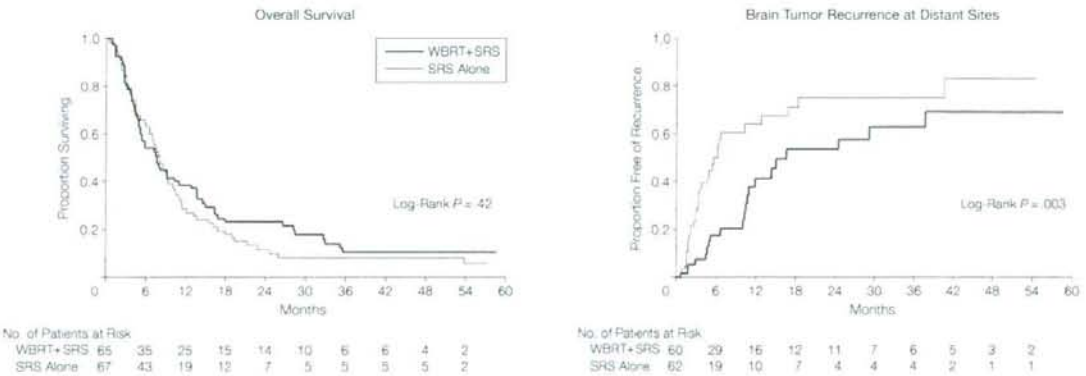

The mean survival time was 7.5 months for patients receiving whole-brain radiation therapy (WBRT) plus stereotactic radiosurgery (SRS) and 8.0 months for patients receiving SRS alone. This difference was not significant ($P=.42$). There was a statistically significant decrease in brain tumor recurrence in the WBRT + SRS group ($P=.003$).

160 eligible patients, of whom 132 (83%) were randomized (65 to WBRT + SRS and 67 to SRS alone) (FIGURE 1). The date of last follow-up was April 2005. The interim analysis was performed with 122 patients (about 60 in each group), which takes into account the possible number of patients with protocol violations. Patient accrual was terminated before the planned final accrual number had been reached because the results of the interim analyses indicated that at least 805 patients were necessary to detect a significant difference in the primary end points. In addition, the numbers of patients appeared sufficient to detect a significant difference in brain tumor recurrence rates: 31 patients in each group were shown to be enough to detect a 30% difference in the median month of 50% brain tumor recurrence (16.2 months with WBRT + SRS vs 5.5 months with SRS alone).

There was no statistical difference between the groups in the baseline characteristics of the patients (Table 1). The median follow-up time was 7.8 months (range, 0.5-58.7 months) for the entire study and 49.2 months (range, 19.6-58.7 months) for survivors. Ninety-two percent of the patients included in the study completed the assigned treatment (Figure 1).

Survival and Cause of Death

By the time of the last follow-up visit in April 2005, 57 patients in the WBRT + SRS group and 62 patients in the SRS-alone group had died. Death was attributed to neurologic causes in 13 patients (22.8%) in the WBRT + SRS group and in 12 patients (19.3%) in the SRS-alone group ($\chi^2 = 0.21$; $P = .64$). The median survival time was 7.5 months with WBRT + SRS and 8.0 months with SRS alone. The higher median survival time with SRS alone was discordant with the 1-year actuarial survival rates of 38.5% (95% CI, 26.7%-50.3%) for the WBRT + SRS group and 28.4% (95% CI, 17.6%-39.2%) for the SRS-alone group ($P = .42$). FIGURE 2A shows that this discordance was due to the crossing of the 2 survival curves. The results of the univariate and multivariate analyses are shown in TABLE 2 and TABLE 3. The number of patients in each institution was too small to allow for a meaningful comparison among institutions. Recursive partition analysis was not included in the multivariate analysis because it is not independent of age and extracranial metastases. Treatment group was not found to be significant in either analysis.

Posttreatment Neurologic Toxicity

A summary of posttreatment neurologic toxicity is given in TABLE 4. Symptomatic acute neurologic toxicity was observed in 4 patients receiving WBRT + SRS and in 8 patients receiv-

Table 2. Univariate Survival Analysis

	No. of Participants	Survival Time, Median (Range), mo	*P* Value
Treatment group			
WBRT + SRS	65	7.5 (0.8-58.7)	.42
SRS alone	67	8.0 (0.5-57.0)	
Age, y			
<65	66	8.9 (0.9-58.7)	.07
≥65	66	6.5 (0.5-55.6)	
Sex			
Male	99	7.1 (0.5-58.7)	.20
Female	33	10.5 (0.8-57.0)	
No. of brain metastases			
1	68	8.6 (1.4-58.7)	.02
2-4	64	7.3 (0.5-55.6)	
Primary tumor site			
Lung	88	8.1 (0.5-58.7)	.33
Other	44	7.1 (0.9-57.0)	
Primary tumor status			
Stable	69	9.2 (0.9-58.7)	<.001
Active	63	6.5 (0.5-53.8)	
Extracranial metastases			
Stable	79	13.3 (1.1-58.7)	<.001
Active	53	6.1 (0.5-55.6)	
RPA			
Class 1	19	16.0 (0.9-58.7)	<.001
Class 2	113	7.5 (0.5-55.6)	
KPS score			
70-80	54	5.0 (0.5-58.7)	<.001
90-100	78	9.2 (0.8-57.0)	
Chemotherapy after brain treatment			
Yes	37	10.1 (1.3-53.8)	.34
No	95	6.8 (0.5-58.7)	

Abbreviations: KPS, Karnofsky Performance Status; RPA, recursive partition analysis; SRS, stereotactic radiosurgery; WBRT, whole-brain radiation therapy.

Table 3. Multivariate Survival Analysis

Variables*	Hazard Ratio (95% CI)	*P* Value
Treatment group (WBRT + SRS)	1.37 (0.93-1.98)	.11
Age (<65 y)	1.48 (1.01-2.16)	.04
No. of brain metastases (1)	1.36 (0.94-1.97)	.10
Primary tumor status (stable)	1.62 (1.11-2.36)	.01
Extracranial metastases (stable)	2.35 (1.55-3.55)	<.001
KPS score (90-100)	1.69 (1.16-2.47)	.007

Abbreviations: CI, confidence interval; KPS, Karnofsky Performance Status; SRS, stereotactic radiosurgery; WBRT, whole-brain radiation therapy.
*Referents appear in parentheses.